

Spectroscopic evidence for a gold-coloured metallic water solution

<https://doi.org/10.1038/s41586-021-03646-5>

Received: 7 October 2020

Accepted: 14 May 2021

Published online: 28 July 2021

 Check for updates

Philip E. Mason^{1,12}, H. Christian Schewe^{1,2,12}, Tillmann Buttersack^{1,2,3,12}, Vojtech Kostal¹, Marco Vitek¹, Ryan S. McMullen³, Hebatallah Ali^{2,4}, Florian Trinter^{2,5,6}, Chin Lee^{2,7,8}, Daniel M. Neumark^{7,8}, Stephan Thürmer⁹, Robert Seidel^{10,11}, Bernd Winter², Stephen E. Bradforth³ & Pavel Jungwirth¹✉

Insulating materials can in principle be made metallic by applying pressure. In the case of pure water, this is estimated¹ to require a pressure of 48 megabar, which is beyond current experimental capabilities and may only exist in the interior of large planets or stars^{2–4}. Indeed, recent estimates and experiments indicate that water at pressures accessible in the laboratory will at best be superionic with high protonic conductivity⁵, but not metallic with conductive electrons¹. Here we show that a metallic water solution can be prepared by massive doping with electrons upon reacting water with alkali metals. Although analogous metallic solutions of liquid ammonia with high concentrations of solvated electrons have long been known and characterized^{6–9}, the explosive interaction between alkali metals and water^{10,11} has so far only permitted the preparation of aqueous solutions with low, submetallic electron concentrations^{12–14}. We found that the explosive behaviour of the water–alkali metal reaction can be suppressed by adsorbing water vapour at a low pressure of about 10^{-4} millibar onto liquid sodium–potassium alloy drops ejected into a vacuum chamber. This set-up leads to the formation of a transient gold-coloured layer of a metallic water solution covering the metal alloy drops. The metallic character of this layer, doped with around 5×10^{21} electrons per cubic centimetre, is confirmed using optical reflection and synchrotron X-ray photoelectron spectroscopies.

Our experiment was realized with a sodium–potassium (NaK) alloy that is liquid at room temperature^{15,16}, dripping at a rate of about one drop every 10 s from a micronozzle into a vacuum chamber with a background water vapour pressure that is tunable up to a fraction of a millibar. With no water vapour in the vacuum chamber, the NaK drops have only a silver metallic sheen (for a representative snapshot see the top left panel of Fig. 1). The lack of visible colour is due to alkali metals possessing neither *d* nor *f* electrons that are subject to optical excitations. Their plasmon frequencies are also far in the ultraviolet region, except for caesium^{9,16,17}.

When the water vapour pressure in the vacuum chamber is increased to $\sim 10^{-4}$ mbar, a sufficient amount of water adsorbs to the surface of the newly formed NaK drops such that their surface layer turns almost immediately gold in colour (Fig. 1). The golden colour persists for up to ~ 5 s, after which, as water continues to adsorb, the colour gradually turns bronze for another 2–3 s (Fig. 1). Eventually, the drop loses its metallic sheen and turns purple/blue and finally white—the latter due to the formation of an alkali hydroxide layer (Fig. 1) as a product of the reaction between the metal and water. The whole process lasts for about 10 s, within which the drop grows and reaches its final size of ~ 5 mm in

diameter. It then falls off the end of the capillary owing to gravitational force, with a new drop starting to evolve immediately afterwards. The transient formation of a gold-coloured drop is completely reproducible for a ‘train’ of hundreds of drops, provided that the water vapour pressure is kept in a relatively narrow range close to the optimal values of about 10^{-4} mbar.

At this pressure, we can estimate using the Langmuir model¹⁸ that the aqueous layer on the NaK drop grows at a rate of ~ 80 monolayers per second; that is, it thickens by about 24 nm s^{-1} . This estimate assumes that an impinging water vapour molecule has a diameter of 0.3 nm and a surface sticking probability of unity (for a schematic picture see Fig. 2). The current situation differs from previous experiments in which a single or very small number of water monolayers were grown on potassium (or by co-adsorption of water with alkali metal on an inert metal substrate) at considerably lower water vapour pressures of $\sim 10^{-6}$ mbar and at cryogenic substrate temperatures of around 100 K (refs.^{19,20}). In those studies, electrons liberated from the alkali metal into the water monolayer transiently formed individual partially hydrated electrons upon annealing, which then reacted towards hydrogen and hydroxide^{19,20}.

¹Institute of Organic Chemistry and Biochemistry, Czech Academy of Sciences, Prague, Czech Republic. ²Molecular Physics, Fritz-Haber-Institut der Max-Planck-Gesellschaft, Berlin, Germany.

³Department of Chemistry, University of Southern California, Los Angeles, CA, USA. ⁴Department of Physics, Faculty of Women for Art, Science and Education, Ain Shams University, Cairo, Egypt. ⁵Photon Science, Deutsches Elektronen-Synchrotron (DESY), Hamburg, Germany. ⁶Institut für Kernphysik, Goethe-Universität Frankfurt, Frankfurt am Main, Germany. ⁷Department of Chemistry, University of California, Berkeley, CA, USA. ⁸Chemical Sciences Division, Lawrence Berkeley National Laboratory, Berkeley, CA, USA. ⁹Department of Chemistry, Graduate School of Science, Kyoto University, Kyoto, Japan. ¹⁰Helmholtz-Zentrum Berlin für Materialien und Energie, Berlin, Germany. ¹¹Department of Chemistry, Humboldt-Universität zu Berlin, Berlin, Germany.

¹²These authors contributed equally: Philip E. Mason, H. Christian Schewe, Tillmann Buttersack. ✉e-mail: pavel.jungwirth@uochb.cas.cz

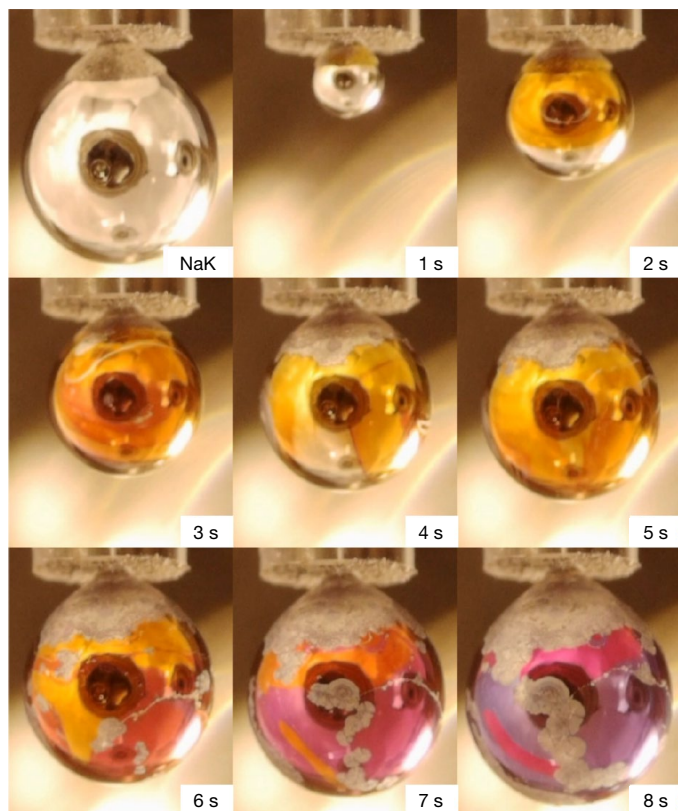


Fig. 1 | A pure NaK drop in vacuum and the time evolution of a NaK drop exposed to water vapour. A fresh NaK drop ejected from a quartz capillary into the vacuum chamber without the presence of water vapour is shown at the top left. This silver drop, with a final diameter of ~ 5 mm, lacks any distinct colour. The series of images shows a second-by-second time evolution of a NaK drop ejected into the vacuum chamber with a background water vapour pressure of $\sim 10^{-4}$ mbar. The snapshots demonstrate the early formation of a gold-coloured layer of a metallic water solution, which (owing to further water adsorption) turns bronze within several seconds and then blue, eventually losing its metallic sheen, with visible white patches of the formed alkali hydroxide.

The key point regarding water adsorption on the alkali metal in the current experiment (Fig. 2) is that the dissolution of electrons and metal cations in water^{11,21} is a much faster process than the growth of the aqueous layer^{18,22}. This aqueous layer building up on the NaK drop is thus heavily doped with electrons and alkali cations. And while the explosive chemistry limits the amount of alkali metal and pure water that can be brought together, we find that multiple layers of the aqueous solution can be grown under our experimental conditions. This growth is a dynamical process, and the formed layer is unlikely to be fully homogeneous. While we hope future studies will investigate the entire evolution of the aqueous surface of the NaK drop in detail, including the metal-to-electrolyte transition^{6,9} and the accompanying chemical transformations, we focus here on the early phase characterized by the golden colour of the drop surface.

Optical and photoelectron spectra

For the gold-coloured drops, we recorded optical reflectance and X-ray photoelectron spectra and compared them with those of pure NaK drops (Fig. 3). Using optical spectroscopy, we imaged the reflected light from a ~ 1 mm² spot at the NaK drop surface and recorded reflection spectra using a commercial UV/visible spectrometer (for details, including calibration, see Methods and Supplementary Information). As mentioned above, pure NaK is colourless and the corresponding

reflection-mode optical spectrum thus shows the spectral intensity distribution of the incandescent lightbulb used to illuminate the sample (black line in Fig. 3a). With water vapour in the chamber, the formation of the gold-coloured aqueous layer on the NaK drop is distinguishable in the spectrum as a prominent broad absorption feature at a wavelength range of 400–600 nm (Fig. 3a, b). A fully quantitative Lorentzian fit to these measured data in energy units is presented in Fig. 4a, yielding a peak at 2.74 eV (corresponding to 452 nm) with a full-width at half-maximum of 0.59 eV.

Analogously to metallic alkali metal–liquid ammonia solutions⁹, we can connect the observed metallic golden colour to the plasmon frequency pertinent to the free electron gas²³ of the metallic water solution. However, unlike the bulk metallic solutions of alkali metals in liquid NH₃, which reflect light below the plasmon frequency and are transparent to light at higher frequencies⁹, here we also observe the absorption of light around the plasmon frequency. We note that in bulk systems, light as transverse electromagnetic radiation cannot for symmetry reasons excite plasmons, which are longitudinal waves²³. This consideration indicates that the metallic water solution formed in our experiments consists of a thin layer, in which optical excitation of a plasmon becomes feasible at around the plasmon frequency²⁴ (see the Supplementary Information for further details).

An interesting feature of the spectrum is that the reflectivity at frequencies above the plasmon absorption band increases again (Fig. 3a, b). The metallic water solution (as with any other simple metal) becomes transparent under radiation of frequencies higher than the plasmon frequency, and hence its reflectivity would not be expected to recover. However, in the case of a thin metallic water layer, high-frequency radiation transmitted through the layer is reflected from the underlying pure NaK, which has a plasmon frequency at only ~ 275 nm (corresponding to 4.5 eV).

Synchrotron radiation X-ray photoelectron spectroscopy experiments were performed in a set-up analogous to the above optical measurements. Photoelectron spectra at photon energy of 330 eV were acquired in the so-called fixed mode that allows simultaneous recording of a 9-eV-wide spectral window with a sampling rate of ~ 0.6 Hz; that is, a spectrum is recorded every 1.6 s (for more details see Methods and Supplementary Information). The spectrum collected from NaK drops ejected into the vacuum chamber in the absence of water vapour (black line in Fig. 3c) is almost identical to that obtained from a pure NaK microjet⁹ (see also Supplementary Information). The main features of the photoelectron spectra of pure NaK are an approximately 2-eV-wide conduction band, with a sharp Fermi edge defining here the zero binding energy, and a Lorentzian-shaped plasmon peak at around 4.5 eV (Fig. 3c and ref. ⁹).

Water vapour adsorption on the NaK drops changes the photoelectron spectrum (yellow line in Fig. 3c) in three distinct ways. First, an additional peak appears at 2.7 eV with a full-width at half-maximum of ~ 0.6 eV on a shallow spectral background (Figs. 3c and 4b), which quantitatively matches the value of the metallic water plasmon energy observed in the optical spectrum (Fig. 3a, b). Second, a new feature appears near the Fermi edge²³, which we interpret as a narrow (~ 1.1 eV) conduction band of the metallic water solution on top of the wider (~ 2 eV) conduction band of pure NaK (Fig. 3c). It is important to reiterate here that the drop is a dynamic system that grows and spins during the measurement. Typically, only part of the region on the drop's surface that is probed by X-rays consists of a metallic water layer, with the remainder being pure NaK alloy. The recorded photoelectron spectrum is therefore a sum of the contributions from the metallic water solution and pure NaK (Fig. 3c). The third change is the appearance of a strong signal at higher binding energies, with an onset around 5.3 eV from the Fermi level. The limited energy window within the fixed-mode data acquisition did not allow for simultaneous measurement of the photoelectron peaks of all of the species present (that is, excess electrons, water, alkali cations and hydroxide anions); nevertheless, we

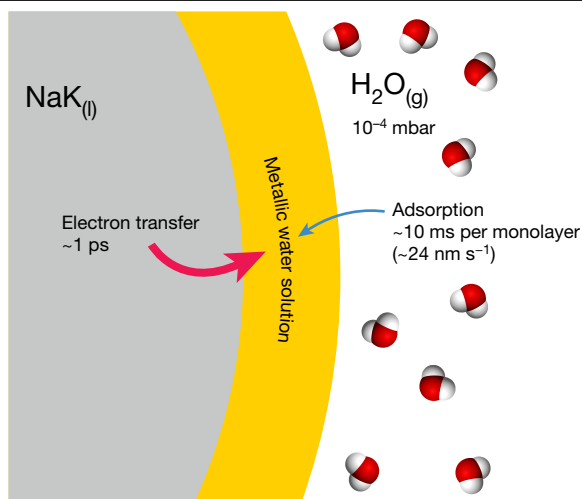


Fig. 2 | Schematic demonstrating the formation of a thin gold-coloured metallic water layer by water vapour adsorption on a NaK drop. The dynamical process is characterized by the much faster dissolution of electrons and alkali cations^{11,21} (thick red arrow) compared with the growth of the aqueous layer^{18,22} (thin blue arrow), which ensures a high concentration of electrons throughout the system. At the same time, chemistry is taking place, leading to the formation of hydroxide and hydrogen.

can clearly see the signal from water in the photoelectron spectra acquired in the sweep mode integrated over the drop lifetime (see Supplementary Information for more details). The observed onset of the spectra in Fig. 3c also occurs in the spectral region where a signal from hydroxide species, both aqueous²⁵ and solid²⁶, should start to appear. As the drop matures, we observe that this onset shifts by about 0.3 eV towards higher binding energies (see Supplementary Information). An analogous shift was noticed previously for increasing concentrations of aqueous hydroxide²⁵. This indicates that before a visible crust of solid alkali hydroxide is formed in the later stages of the drop's development, hydroxide seems to be dissolved in the thin layer of metallic water.

The decomposition of the photoelectron spectrum into contributions from the metallic water solution and NaK, with conduction bands and plasmons fitted using the free electron gas model assuming a Lorentzian shape of the plasmon peaks, is presented in Fig. 4b (see Supplementary Information for more details). Despite its simplicity and just a single adjustable parameter (the density of free electrons), it is remarkable how well the model fits the experimental data. The value of the obtained free electron density is about $5 \times 10^{21} \text{ cm}^{-3}$, which corresponds to a concentration of ~18 mole per cent metal (MPM). This estimated value for the metallic aqueous solutions of sodium and potassium is probably close to the saturation limit, as it is consistent with the solubilities of these alkali metals in liquid ammonia reaching ~20 MPM (with the electrolyte-to-metal transition occurring at around 1–5 MPM)⁶. We also note that the free electron density of the metallic water solution is about three times lower than that of pure NaK (ref. ⁹), which is in line with the UV-to-visible shift of the plasmon peak and a conduction band of about half of the width of that of pure NaK (Fig. 4b).

Discussion and conclusions

We have shown here that exposing NaK drops to a water vapour pressure of 10^{-4} mbar leads to the almost immediate formation of a gold-coloured layer of a metallic water solution. The gold colour cannot be due to interference effects since it appears when the layer is more than an order of magnitude thinner than the corresponding wavelength region of 400–600 nm. Moreover, we do not observe any red-to-blue colour shift as would be expected in the case of interference

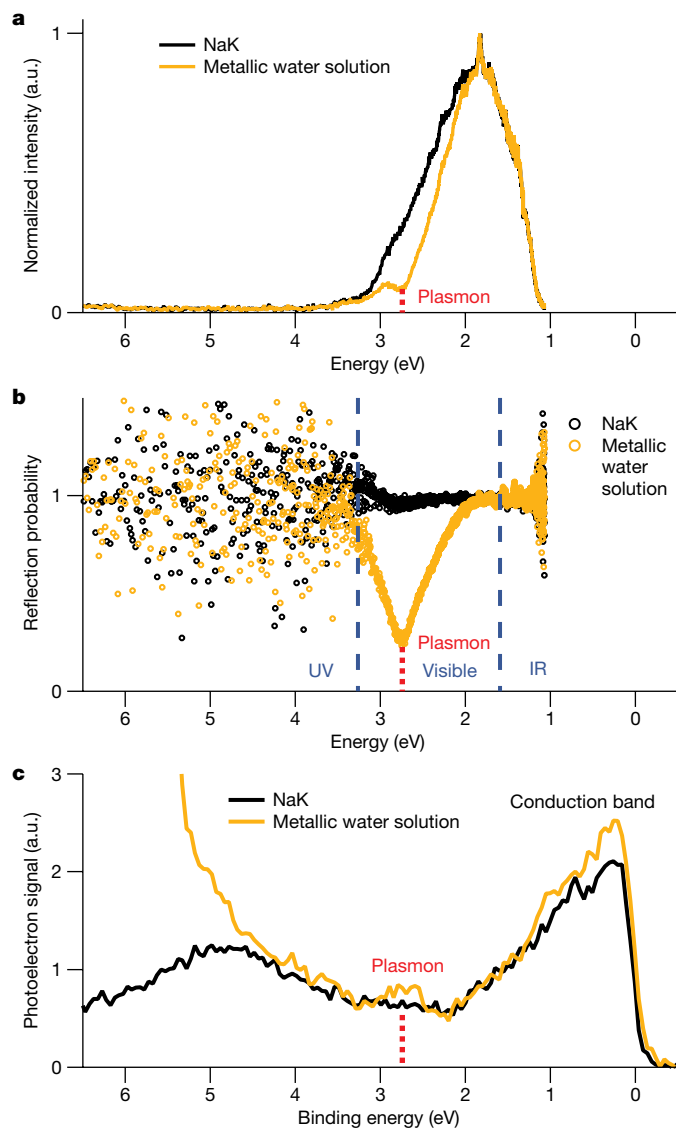


Fig. 3 | Spectroscopic signatures of the metallic water solution from optical and X-ray photoelectron spectroscopy. a–c, Optical reflection spectra before and after subtraction of the lamp spectrum (a, b) and photoelectron spectra (c) of a metallic water solution (gold) compared with pure NaK (black). **a,** The spectrum of the colourless NaK drop reflects the spectral characteristics of the illuminating lamp. **b,** When the lamp spectrum is subtracted, a largely flat spectrum is obtained for this system with a prominent plasmonic absorption peak of the metallic water layer in the visible region of the spectra. **c,** The emerging features in the photoelectron spectrum upon exposure to a water vapour pressure of 10^{-4} mbar encompass a new plasmon peak and a narrow conduction band next to the Fermi edge. We also observe a signal from the produced hydroxide as the signal rise above -4.5 eV. Note that the red dashed line in all panels marks the position of the plasmon peak.

from a layer growing to a thickness approaching the wavelengths of the blue edge of the visible spectrum. Our observations confirm that, instead, the gold colour with its characteristic sheen is a signature of the metallic character of the aqueous surface layer.

The relatively long lifetime of several seconds of the metallic water solution layer is partly due to the underlying alkali metal providing excess electrons in a quasi-steady-state manner; this is similar to our earlier experiments, where placing a NaK alloy next to a water drop led to the transient formation of a blue electrolyte layer of hydrated electrons at elevated temperature¹³. In addition, it is plausible that hydrated electrons become less reactive and thus longer-lived upon

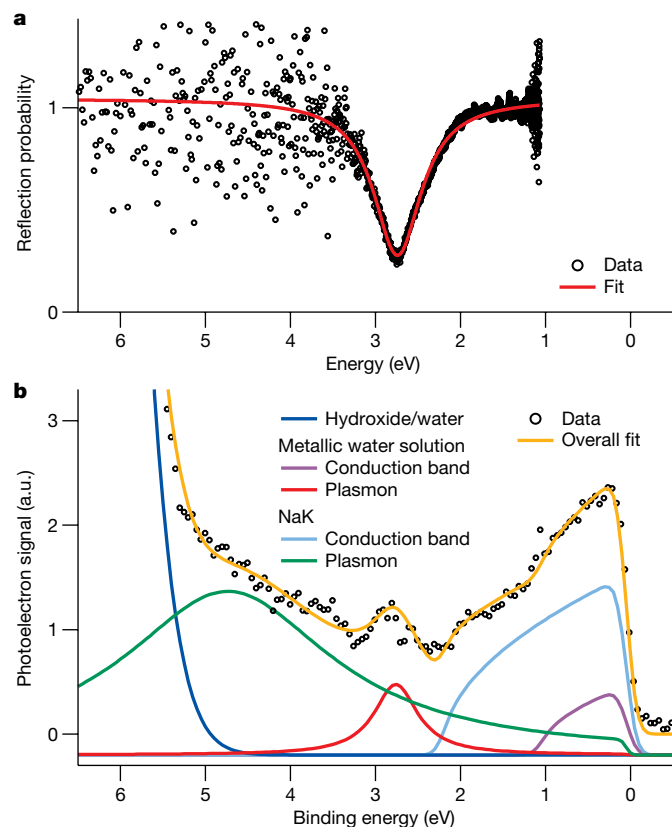


Fig. 4 | Fits to the experimental data employing a free electron gas model. a, A Lorentzian fit to the plasmonic absorption feature in the optical reflection spectrum yields a broad peak at 2.74 eV. **b,** Fits to averaged photoelectron spectra of NaK drops exposed to a water vapour pressure of 10^{-4} mbar, namely to the plasmon peaks (obtained by Lorentzian functions) and conduction bands of both NaK and a metallic water solution using the free electron gas model. The formation of the gold-coloured metallic water layer is accompanied by the appearance of a plasmon peak at ~ 2.7 eV and a 1.1-eV-wide conduction band with a sharp Fermi edge at 0 eV.

delocalization in the metallic regime. This effect could be rationalized by the fact that there is a better chance for localized hydrated electrons to react with adjacent water molecules than for delocalized electrons in the conduction band of the metallic solution. The lifetime of dilute localized hydrated electrons is sub-millisecond²⁷, whereas in the experiments presented here the metallic water layer persists for seconds. However, the presence of a hydroxide signal in the photoelectron spectra indicates that chemical transformations removing electrons start early in the process. The metallic water solution should thus be viewed as a dynamically evolving system comprising a high concentration of excess electrons that form a conduction band and alkali metal cations. As chemistry proceeds during drop development, hydroxide anions and hydrogen form and give rise to an increasingly concentrated aqueous hydroxide solution and the growth of solid hydroxide. Consistent with earlier observations of a blue colour of electrons in strongly alkaline amorphous ices^{28,29}, this effect—together with further water adsorption—is probably causing the change in colour to purple/blue as the drop matures (Fig. 1).

This study demonstrates that by adsorbing water vapour on a NaK drop the vigorous (even explosive) chemical reactivity can be

suppressed sufficiently for visual observation and spectroscopic characterization of the formed gold-coloured layer of metallic water solution. In this way, one is able to bypass the need to use unrealistically high pressures to metallize water.

Online content

Any methods, additional references, Nature Research reporting summaries, source data, extended data, supplementary information, acknowledgements, peer review information; details of author contributions and competing interests; and statements of data and code availability are available at <https://doi.org/10.1038/s41586-021-03646-5>.

- Hermann, A., Ashcroft, N. W. & Hoffmann, R. High pressure ices. *Proc. Natl Acad. Sci. USA* **109**, 745–750 (2012).
- Dubrovinsky, L., Dubrovinskaia, N., Prakapenka, V. B. & Abakumov, A. M. Implementation of micro-ball nanodiamond anvils for high-pressure studies above 6 Mbar. *Nat. Commun.* **3**, 1163 (2012).
- Cavazzoni, C. et al. Superionic and metallic states of water and ammonia at giant planet conditions. *Science* **283**, 44–46 (1999).
- Mattsson, T. R. & Desjarlais, M. P. Phase diagram and electrical conductivity of high energy-density water from density functional theory. *Phys. Rev. Lett.* **97**, 017801 (2006).
- Millot, M. et al. Nanosecond X-ray diffraction of shock-compressed superionic water ice. *Nature* **569**, 251–255 (2019).
- Zurek, E., Edwards, P. P. & Hoffmann, R. A molecular perspective on lithium-ammonia solutions. *Angew. Chem. Int. Ed.* **48**, 8198–8232 (2009).
- Thompson, J. C. *Electrons in Liquid Ammonia* (Clarendon Press, 1976).
- Lodge, M. et al. Multielement NMR studies of the liquid-liquid phase separation and the metal-to-nonmetal transition in fluid lithium- and sodium-ammonia solutions. *J. Phys. Chem. B* **117**, 13322–13334 (2013).
- Buttersack, T. et al. Photoelectron spectra of alkali metal-ammonia microjets: from blue electrolyte to bronze metal. *Science* **368**, 1086–1091 (2020).
- Hutton, A. T. Dramatic demonstration for a large audience: the formation of hydroxyl ions in the reaction of sodium with water. *J. Chem. Educ.* **58**, 506 (1981).
- Mason, P. E. et al. Coulomb explosion during the early stages of the reaction of alkali metals with water. *Nat. Chem.* **7**, 250–254 (2015).
- Young, R. M. & Neumark, D. M. Dynamics of solvated electrons in clusters. *Chem. Rev.* **112**, 5553–5577 (2012).
- Mason, P. E., Buttersack, T., Bauerecker, S. & Jungwirth, P. A non-exploding alkali metal drop on water: from blue solvated electrons to bursting molten hydroxide. *Angew. Chem. Int. Ed.* **55**, 13019–13022 (2016).
- Suzuki, T. Ultrafast photoelectron spectroscopy of aqueous solutions. *J. Chem. Phys.* **151**, 090901 (2019).
- Alchagirov, B. B. et al. Surface tension and adsorption of components in the sodium-potassium alloy systems: effective liquid metal coolants promising in nuclear and space power engineering. *Inorg. Mater. Appl. Res.* **2**, 461–467 (2011).
- Addison, C. C. *The Chemistry of Liquid Alkali Metals* (Wiley, 1984).
- Citrin, P. H. High-resolution X-ray photoemission from sodium metal and its hydroxide. *Phys. Rev. B* **8**, 5545–5556 (1973).
- Lueth, H. *Surfaces and Interfaces of Solid Materials* (Springer, 1997).
- Kiskinova, M., Pirug, G. & Bonzel, H. P. Adsorption and decomposition of H₂O on a K-covered Pt(111) surface. *Surf. Sci.* **150**, 319–338 (1985).
- Blass, P. M., Zhou, X. L. & White, J. M. Coadsorption and reaction of water and potassium on Ag(111). *J. Phys. Chem.* **94**, 3054–3062 (1990).
- Nachtrieb, N. H. Self-diffusion in liquid metals. *Adv. Phys.* **16**, 309–323 (1967).
- Ketteler, G. et al. The nature of water nucleation sites on TiO₂(110) surfaces revealed by ambient pressure X-ray photoelectron spectroscopy. *J. Phys. Chem. C* **111**, 8278–8282 (2007).
- Kittel, C. *Introduction to Solid State Physics* (Wiley, 2005).
- Abelès, F., Borensztein, Y., Decrescenzi, M. & Lopezrios, T. Optical evidence for longitudinal-waves in very thin Ag layers. *Surf. Sci.* **101**, 123–130 (1980).
- Winter, B., Faubel, M., Vacha, R. & Jungwirth, P. Behavior of hydroxide at the water/vapor interface. *Chem. Phys. Lett.* **474**, 241–247 (2009).
- Bonzel, H. P., Pirug, G. & Winkler, A. Adsorption of H₂O on potassium films. *Surf. Sci.* **175**, 287–312 (1986).
- Hart, E. J. & Boag, J. W. Absorption spectrum of hydrated electron in water and in aqueous solutions. *J. Am. Chem. Soc.* **84**, 4090–4095 (1962).
- Barzynski, H. & Schulte-Frohlinde, D. On the nature of the electron traps in alkaline ice. *Z. Naturforsch. A* **22**, 2131–2132 (1967).
- Keivan, L. Solvated electron structure in glassy matrices. *Acc. Chem. Res.* **14**, 138–145 (1981).

Publisher's note Springer Nature remains neutral with regard to jurisdictional claims in published maps and institutional affiliations.

© The Author(s), under exclusive licence to Springer Nature Limited 2021

Methods

The liquid NaK alloy was made by mixing equimolar amounts of solid sodium and potassium. Further details are provided in ref.¹¹ and all of the experimental procedures are detailed in Supplementary Information and Supplementary Video 1. To acquire both the optical and photoelectron spectra, we used our modified microjet set-up described in ref.³⁰ to produce drops of NaK and added a water supply line to transfer water vapour at pressures varying from 10^{-5} to 2×10^{-4} mbar into our vacuum chamber.

The optical reflection measurements were conducted at IOCB Prague with spectra recorded every 0.1–0.3 s using an AvaSpecULS 2048 spectrometer. We synchronized the saving of the time stamp of each spectrum by recording a video where the image of the drop taken with a CCD camera is shown together with the current time to directly relate the sampled spectra to the size and colour of the NaK drop at a given moment. First, we took reference reflection spectra of pure NaK drops, the surfaces of which are highly reflective in the infrared and visible parts of the electromagnetic spectrum. Next, water vapour was transferred into the vacuum chamber via a tube from a water reservoir with the amount of vapour controlled using a needle valve. We found that NaK drops turned golden for several seconds within a pressure range of 6×10^{-5} to 2×10^{-4} mbar, with the optimal performance at $\sim 10^{-4}$ mbar. The spectra taken at this water vapour pressure were normalized using the reflection spectra of pure NaK.

X-ray photoelectron spectroscopy measurements were performed using the SOL³PES set-up³¹ connected to the U49-2_PGM-1 beamline³² of the synchrotron radiation facility BESSY II in Berlin. Similarly to the optical measurements, experiments were performed under vacuum conditions (10^{-5} mbar) with or without the presence of water vapour at a pressure of $\sim 10^{-4}$ mbar. The upper parts of the NaK drops were irradiated by horizontally polarized soft-X-ray light. Water vapour was directed onto the same spot on the surface where the X-ray photons hit the drop. The emitted photoelectrons were detected by a ScientaOmicron R4000 HiPP-2 hemispherical electron analyser mounted in the same plane as the polarization axis. Valence photoelectron spectra were measured at a photon energy of 330 eV using a pass energy of 100 eV. This large pass energy allowed us to detect within the fixed-mode setting of the electron analyser a 9-eV-wide kinetic energy window in one shot, which was enough to record the conduction band with its Fermi edge and the plasmon features, as well as the onset of the hydroxide peak. A sampling rate of 0.6 Hz was chosen to guarantee a sufficient time resolution as well as a good enough signal-to-noise ratio.

Data availability

The datasets generated during the current study are available as Source Data or are available from the corresponding author upon reasonable request. Source data are provided with this paper.

Code availability

Data-processing and fitting results can be generated using numerical methods described in Methods and Supplementary Information and developed computer codes that are available from the corresponding author upon reasonable request.

30. Buttersack, T. et al. Deeply cooled and temperature controlled microjets: liquid ammonia solutions released into vacuum for analysis by photoelectron spectroscopy. *Rev. Sci. Instrum.* **91**, 043101 (2020).
31. Seidel, R., Pohl, M. N., Ali, H., Winter, B. & Aziz, E. F. Advances in liquid phase soft-X-ray photoemission spectroscopy: a new experimental setup at BESSY II. *Rev. Sci. Instrum.* **88**, 073107 (2017).
32. Sawhney, K. J. S., Senf, F. & Gudat, W. PGM beamline with constant energy resolution mode for U49-2 undulator at BESSY-II. *Nucl. Instrum. Methods Phys. Res. Sect. A* **467**, 466–469 (2001).

Acknowledgements P.J. acknowledges support from the European Regional Development Fund (project ChemBioDrug number CZ.02.1.01/0.0/0.0/16_019/0000729). D.M.N. and C.L. acknowledge support from the Director of the Office of Basic Energy Science, Chemical Sciences Division of the US Department of Energy under contract number DE-AC02-05CH11231. D.M.N., C.L. and P.J. thank the Alexander von Humboldt Foundation for support. S.E.B., T.B. and R.S.M. are supported by the US National Science Foundation (CHE-1665532). P.E.M. acknowledges support from the viewers of his YouTube popular science channel. M.V. acknowledges support from the Charles University in Prague and from the International Max Planck Research School in Dresden. S.T. acknowledges support from JSPS KAKENHI grant number JP18K14178. R.S. acknowledges the German Research Foundation (DFG) for an Emmy-Noether Young-Investigator stipend (DFG, project SE 2253/3-1). F.T. and B.W. acknowledge support from the MaxWater initiative of the Max-Planck-Gesellschaft. All authors thank the staff of the Helmholtz-Zentrum Berlin for their support during the beamtime at BESSY II.

Author contributions P.E.M., H.C.S., T.B., B.W., S.E.B. and P.J. designed the experiments. P.E.M., H.C.S., T.B., B.W., H.A., V.K., M.V., F.T., C.L., D.M.N., R.S. and P.J. performed the experiments, and P.E.M., H.C.S., T.B., B.W., S.E.B., R.S.M., C.L., R.S., S.T. and P.J. analysed the obtained data. P.J. wrote the main paper, and H.C.S. and P.J. wrote the Supplementary Information, both with critical feedback from all co-authors. P.E.M. produced Supplementary Video 1.

Competing interests The authors declare no competing interests.

Additional information

Supplementary information The online version contains supplementary material available at <https://doi.org/10.1038/s41586-021-03646-5>.

Correspondence and requests for materials should be addressed to P.J.

Peer review information *Nature* thanks Christoph Salzmann and the other, anonymous, reviewer(s) for their contribution to the peer review of this work. Peer reviewer reports are available.

Reprints and permissions information is available at <http://www.nature.com/reprints>.